Bioelectrochemistry 140 (2021) 107813

Contents lists available at ScienceDirect

Bioelectrochemistry

journal homepage: www.elsevier.com/locate/bioelechem

Cell-based electrochemical cytosensor for rapid and sensitive evaluation of the anticancer effects of saponin on human malignant melanoma cells

Won Hur, Seong Eun Son, Seong Nyeon Kim, Gi Hun Seong *

Department of Bionano Engineering, Center for Bionano Intelligence Education and Research, Hanyang University, Ansan 426-791, South Korea

ARTICLE INFO

Article history:
Received 5 February 2021
Received in revised form 25 March 2021
Accepted 28 March 2021
Available online 31 March 2021

Keywords:
Cell-based biosensor
Cytosensor
Electrochemical detection
Human skin malignant melanoma
Saponin
Anticancer drug assessment

ABSTRACT

Discovering new anticancer agents and analyzing their activities is a vital part of drug development, but it requires a huge amount of time and resources, leading to the increasing demands for more-effective techniques. Herein, a novel and simple cell-based electrochemical biosensor, referred to as a cytosensor, was proposed to investigate the electrochemical behavior of human skin malignant melanoma (SK-MEL28) cells and the anticancer effect of saponin on cell viability. To enhance both electrocatalytic properties and biocompatibility, gold nanoparticles were electrochemically deposited onto a conductive substrate, and poly-L-lysine was further added to the electrode surface. Electric signals from SK-MEL28 cells on the electrodes were obtained from cyclic voltammetry and differential pulse voltammetry. The cathodic peak current was proportional to the cell viability and showed a detection range of 2,880–40,000 cells per device with an excellent linear cell number-intensity relationship (R^2 = 0.9952). Furthermore, the anticancer effect of saponin on SK-MEL28 cells was clearly established at concentrations higher than 20 μM, which was highly consistent with conventional assays. Moreover, the developed electrochemical cytosensor for evaluating anticancer effects enabled rapid (<2 min), sensitive (LOQ: 2,880 cells/device), and non-invasive measurements, thus providing a new avenue for assessing the anticancer drugs in vitro.
© 2021 Elsevier B.V. All rights reserved.

1. Introduction

Globally, cancer is the second leading cause of death and is considered a crucial public health problem [1]. Millions of people struggle against cancer, and a third of them die every year. Specifically, malignant skin melanoma, which is the most aggressive form of skin cancer, has to be treated quickly due to its potential to spread to other parts of the body and become a life-threatening emergency within 6 weeks of cancer diagnosis [2]. Proper treatment in the early stage is very important to improve the survival rate. Even with recent advancements, which include surgical resection, cold atmospheric plasma, targeted therapy [3,4], and immunotherapy [5,6], skin melanoma is notoriously difficult to treat when it starts to spread beyond its original site. That is, a well-established anticancer therapy must be developed with reduced side effects such as illness recurrence, drug resistance, and severe damage to the normal cells. Phytochemicals, which are chemical compounds from natural plants or animals (including alkaloids, saponin, polyphenols, terpenoids, and steroids) are well known to inhibit the growth of many cancer cells [7–9]. Among them, saponin has been considered as a promising agent for cancer research and development due to its significant anticancer activities such as anti-metastasis, anti-angiogenesis, anti-proliferation, and reversal of multi-drug resistance effects [7,10–12]. It also has been reported to reduce the side effects of several existing therapies. The antiproliferative activity of saponin against melanoma is associated with the inhibition of the JAK/STAT pathway, resulting in tumor cell growth suppression [7]. Also, saponins are known to increase the efficiency of several chemotherapeutic drugs [13].

Currently, cell counting/staining methods such as the thiazolyl blue tetrazolium bromide (MTT) assay, Cell Counting Kit-8 (CCK-8), and trypan blue exclusion have been commonly used to detect cell viability and study the efficiency of anticancer drugs. Those assays, however, have critical challenges that cause irreversible damage to cells and require complicated and time-consuming sampling processes, expensive robotic equipment, and invasive chemical reagents for measuring cellular metabolic activities. Those assays also have a shortcoming for assessing the efficiency

Abbreviations: AuNPs, gold nanoparticles; FTO, fluorine-doped tin oxide; MTT, thiazolyl blue tetrazolium bromide; PLL, poly-L-lysine; CV, cyclic voltammetry; CC, chronocoulometry; DPV, differential pulse voltammetry; PBS, phosphate buffered saline; SEM, scanning electron microscopy; DI, deionized; DMSO, dimethyl sulfoxide; MEM, minimum essential medium; FBS, fetal bovine serum; TE, trypsin-EDTA; LOQ, limit of quantification.

* Corresponding author.
E-mail address: ghseong@hanyang.ac.kr (G.H. Seong).

https://doi.org/10.1016/j.bioelechem.2021.107813
1567-5394/© 2021 Elsevier B.V. All rights reserved.

of colored drugs due to a possibility of signal interference at the specific wavelength. For these reasons, alternative sensing techniques for in vitro toxicological assessment such as those based on electrochemistry [14,15], optics [14,16], and quartz crystal microbalances [17,18] have been vigorously investigated. Among these methods, the electrochemical strategy, which features fast response time, real-time monitoring, easy miniaturization, high sensitivity, and cost effectiveness have been utilized to evaluate anticancer activities for the purpose of reducing the time and cost in the early stage of drug development [19–23]. In particular, an electrochemical cell-based biosensor, called a cytosensor, has been actively developed for the last decade as a rapid, sensitive, label-free, and non-invasive technique to monitor the various cell types (e.g., cancer cells and pluripotent stem cells) [22,24]. For example, voltammetric behavior of cells can be utilized for rapid real-time monitoring due to its good dynamic kinetic properties for determining electrochemical redox activity of proteins [23–29]. Because of the various biochemical reactions, including the oxidation/reduction of several biomolecules (such as redox proteins and metalloproteins inside cells), distinct electrochemical redox signals for each cell type were found to be generated and measured at specific potentials, and these can be used to investigate the sensitivity of cancer cells to the anticancer drugs.

Herein, we report an electrochemical cytosensor platform which enables sensitive and fast assessment of the anticancer effects of saponin on the most aggressive form of skin cancer, called human malignant melanoma (SK-MEL28). Gold nanoparticles (AuNPs) were electrochemically deposited onto fluorine-doped tin oxide (FTO) electrodes to enhance their electrocatalytic properties. The AuNPs/FTO platforms were further modified with biocompatible poly-L-lysine (PLL) to promote cell adhesion and growth. With a combination of the nano and biocompatible materials, the sensor platform developed for evaluating anticancer activity has achieved direct electron transfer between immobilized cancer cells and the manufactured electrode surface and improved the selectivity and sensitivity of the cytosensor. Consequently, the electrical signal intensity of SK-MEL28 cells showed clear linearity ($R^2 = 0.9952$) relative to the number of cells, suggesting that the intensity of the peak current of the cytosensor can be used to detect the number of SK-MEL28 cells and monitor the anticancer effects of various drugs, thus being a simple and effective way to study the evaluation of novel drug candidates and promote the development of powerful anticancer reagents.

2. Materials and methods

2.1. Materials

Gold (III) chloride trihydrate ($HAuCl_4$), PLL solution (0.01%), MTT, dimethyl sulfoxide (DMSO), trypan blue, and saponin were purchased from Sigma-Aldrich (St. Louis, MO, USA). FTO glass slides were obtained from Omni Science (Yong-in, South Korea). Minimum Essential Medium (MEM) was from Gibco (USA). Phosphate buffered saline (1X, PBS), fetal bovine serum (FBS), penicillin-streptomycin solution (100X), and trypsin-EDTA (TE) solution were obtained from Welgene (Gyeongbuk, South Korea). Calcein-AM and ethidium homodimer-1 (EthD-1) were acquired from Invitrogen (Carlsbad, CA, USA). All chemicals were of analytical grade.

2.2. Cell chip fabrication

The sensing platform of electrochemical cytosensors was composed of FTO glass (20 × 20 mm) and a polystyrene well (diameter: 10 mm). FTO glass slides were sequentially washed with a 1% triton X-100 solution, 70% ethanol, and deionized (DI) water for 10 min and dried with nitrogen gas. A polystyrene well structure was designed using AutoCAD 2019 software (Autodesk Inc.) and were fabricated with a laser cutting machine (C40 60 W, Coryart, South Korea). Due to its one-sided adhesive property, the polymer structure was firmly attached on the FTO glass. Next, the fabrication of a AuNP layer on the FTO electrode was carried out using electrochemical deposition. An AuNP solution (0.5 M H_2SO_4 containing 5 mM $HAuCl_4$) was filled into the prepared well-electrode platform. A cyclic voltammetry (CV) measurement was performed in a potential range of 1.2 V to −0.6 V, and the Epc potential was chosen as the working potential for electrodeposition of AuNPs using chronocoulometry (CC). After washing with DI water, AuNP-FTO was coated with a 0.01% PLL solution for 30 min at room temperature. The PLL solution was removed and washed with DI water 3 times right before seeding 500 μL of the cell suspension on the chip.

2.3. Cell culture

A human malignant melanoma cell line (SK-MEL28, 30072; Korean Cell Line Bank, Seoul, South Korea) was cultured in MEM supplemented with 10% FBS and 1% penicillin-streptomycin. Cells were maintained at 37 °C in a humidified atmosphere of 5% CO_2. The culture medium was changed every 2 days. Cells were passaged using a TE solution, and the detached cells were transferred to the Styrofoam well-FTO glass structure to a concentration of less than 8.0×10^4 cells/mL. Cell concentrations were determined using a disposable hemocytometer (INCYTO, Cheonan, South Korea). The morphologies of the cells were analyzed using an optical microscope (IX71, Olympus, Japan).

2.4. Electrochemical detection

Electrochemical experiments for CV and DPV measurements were carried out using a CHI660C workstation (CH Instruments Inc., USA). A three-electrode system was composed of the fabricated FTO chip as the working electrode (WE), Ag/AgCl (saturated in 3 M NaCl) as the reference electrode (RE), and a platinum wire as the counter electrode (CE).

2.5. Anticancer effect assay

SK-MEL28 cells were cultured on a PLL/AuNPs/FTO chip under the same conditions in vitro. At 2DIV, the cells were treated with medium containing saponin for 24 h. For the CV and DPV signal measurement, the cell culture medium was removed and 1X PBS (pH 7.4) was used as an electrolyte.

2.6. Cell viability assay

A MTT assay was conducted by culturing cells in a multi-well plate to observe cellular viability after drug treatment and compare the results of the conventional colorimetric assay with the electrochemical method. The MTT working solution was prepared and added to each well to a final concentration of 0.5 mg/mL. After the cells were further cultured for 4 h at 37 °C, DMSO was added to each well, and the absorbance was measured on a microplate reader (Synergy HTX, BioTek, South Korea) at 540 nm. In addition, live/dead cell staining was carried out to distinguish between live and dead cells. Then, 2 μM calcein-AM and 4 μM EthD-1 in culture media were added to the cells for 30 min at 37 °C in a dark incubator. Stained cells were visualized and captured using a fluorescent microscope (IX81, Olympus, Japan). Based on the enzyme activity

and plasma membrane integrity, live cells exhibited green fluorescence, and the dead cells showed red fluorescence.

2.7. Statistics

Graphical data were presented as mean values ± standard deviation (s.d.) with three replicates (N = 3). The statistical significance of the difference between the two groups was determined by the unpaired student's *t*-test. A *p* value of less than 0.05 (*p < 0.05) was considered statistically significant. Data were analyzed using the statistical software OriginPro 2016 and SigmaPlot 10.0.

3. Results and discussion

3.1. Voltammetric behavior of skin melanoma cells on the fabricated electrode

We designed an electrochemical cytosensor based on a conventional three-electrode system (Fig. 1A). The sensing platform was composed of a RE (Ag/AgCl), a CE (Pt wire), and a WE (FTO-doped glass substrate with a polystyrene chamber on it). SK-MEL28 skin melanoma cells were plated onto the fabricated electrode and maintained for 2 days. After that, a specific cathodic peak potential (Epc) and a peak current (Ipc) of skin melanoma SK-MEL28 cells were first determined by measuring the CV signal of the cells cultured on each of the fabricated electrodes (Fig. 1B). CV measurements were carried out using a PBS buffer (pH 7.4) as an electrolyte, and a reductive peak at around −0.064 V (vs. Ag/AgCl) was observed at a scan rate of 100 mV/s. The redox signal obtained from the living cells can be explained by the existence of several biomolecules such as intracellular redox enzymes and metalloproteins in the cell membrane, which participate in the biochemical redox reaction. In previous reports, it has been considered that the harmony of these biomolecules in cells generates a cell type-specific bioelectrical signal, especially for certain cell types such as pluripotent stem cells and cancer cells and guides the detection of cell viability through electrochemical measurement [23,30]. For example, redox enzymes such as matrix metalloproteinases are present in higher amounts and more activated form in malignant cancer cells than in normal cells. It has been reported that these redox enzymes generate distinctive electrochemical signals at specific potentials [31,32]. Likewise, numerous enzymes such as matrix metalloproteinases and phosphatases in SK-MEL28 cells serve as redox-active centers in oxidation and reduction reactions [24]. Therefore, when these redox centers are close enough to the electrode, direct electron transfer between the cell and electrode surface generates, which is distinct from that in the bulk medium [33].

As shown in Fig. 1B, there were no redox peaks of the cells grown on the bare FTO electrode and cells grown on PLL-treated FTO electrode in the potential range of −0.3 to +0.3 V. The cancer cells did not show any detectable electrochemical signal at the electrode without AuNPs. However, the SK-MEL28 cells attached to the AuNPs-modified FTO electrode exhibited a significantly increased voltammetric signal. It can be attributed to an excellent attachment of cells on the surface of AuNPs and an electrical signal enhancement by a high conductivity of AuNPs [34,35]. These results show that the electrodeposition of AuNPs could improve the poor electrocatalytic properties of the bare FTO substrate and enhance the sensitivity of the cell-based electrochemical biosensor. The electrocatalytic activity of the fabricated electrode was further promoted by adding a biocompatible conducting polymer, PLL, onto the AuNP-deposited electrode substrate. However, in the PLL-Au-FTO electrodes without cells, no signal was measured, showing that the generated electrochemical signal is attributed to the existence of the cells on the electrode substrate (Fig. S1).

3.2. AuNP deposition and PLL treatment for enhanced electric signals

AuNPs were electrochemically deposited onto the FTO substrate using CV and CC techniques (Fig. 2) to enhance the electrocatalytic properties of the electrodes for cell type-specific electrochemical signal detection. We investigated the morphologies of the gold nanostructure-FTO electrodes based on deposition time and the biocompatibility of the platforms in the presence of cells. Fig. 2A-C show scanning electron microscopy (SEM) images of the sphere-shaped AuNPs electrochemically formed on the transparent FTO electrodes. The sizes of AuNPs for the deposition time of 10, 30, and 90 s were 147, 151, and 168 nm, respectively. Based on the SEM images of the substrates, sparsely deposited AuNPs were discovered on the electrode surfaces with deposition times of 10 s (Fig. 2A). On the other hand, the electrochemical deposition of gold for 30 s could create dense and homogeneous nanostructures on the FTO surface (Fig. 2B). However, random aggregates of larger AuNPs were discovered on the electrode surfaces with a deposition time of 90 s (Fig. 2C). AuNP deposition times exceeding 90 s were not examined because no more particles could be added to the surface beyond the saturation level due to geometrically limited conditions. Fig. 2D-F indicate the optical images of the SK-MEL28 cells incubated on the fabricated AuNPs-FTO electrodes with AuNP deposition times of 10, 30, and 90 s, respectively. The results showed that there were no specific side-effects caused by gold nanostructures towards SK-MEL28 cell proliferation on each

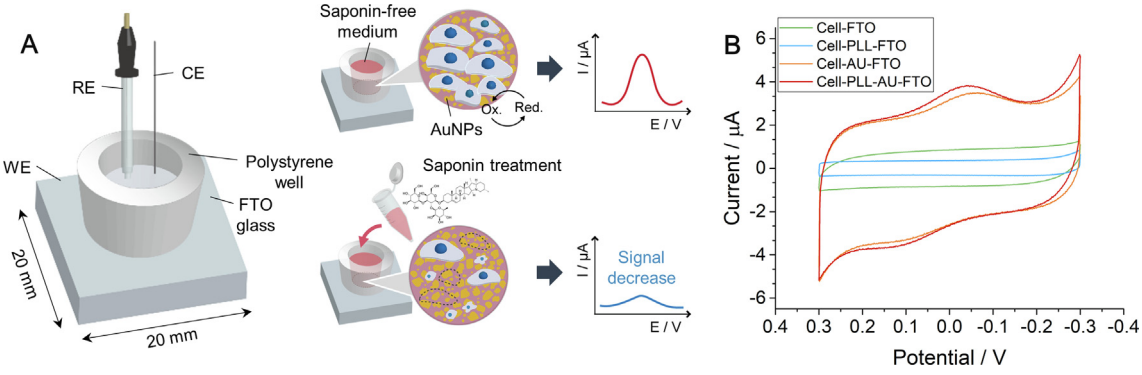

Fig. 1. (A) A schematic illustration of the SK-MEL28 cell-based electrochemical biosensing platform based on the three-electrode system and a working principle for the assessment of anticancer effects of saponin. (B) Cyclic voltammograms of SK-MEL28 cell-FTO (green line), cell-PLL-FTO (blue line), cell-Au-FTO (orange line), and cell-PLL-Au-FTO (red line) electrodes in pH 7.4 PBS buffer. Cell concentration: 4.0 × 10^4 cells/mL, scan rate: 100 mV s^{-1}.

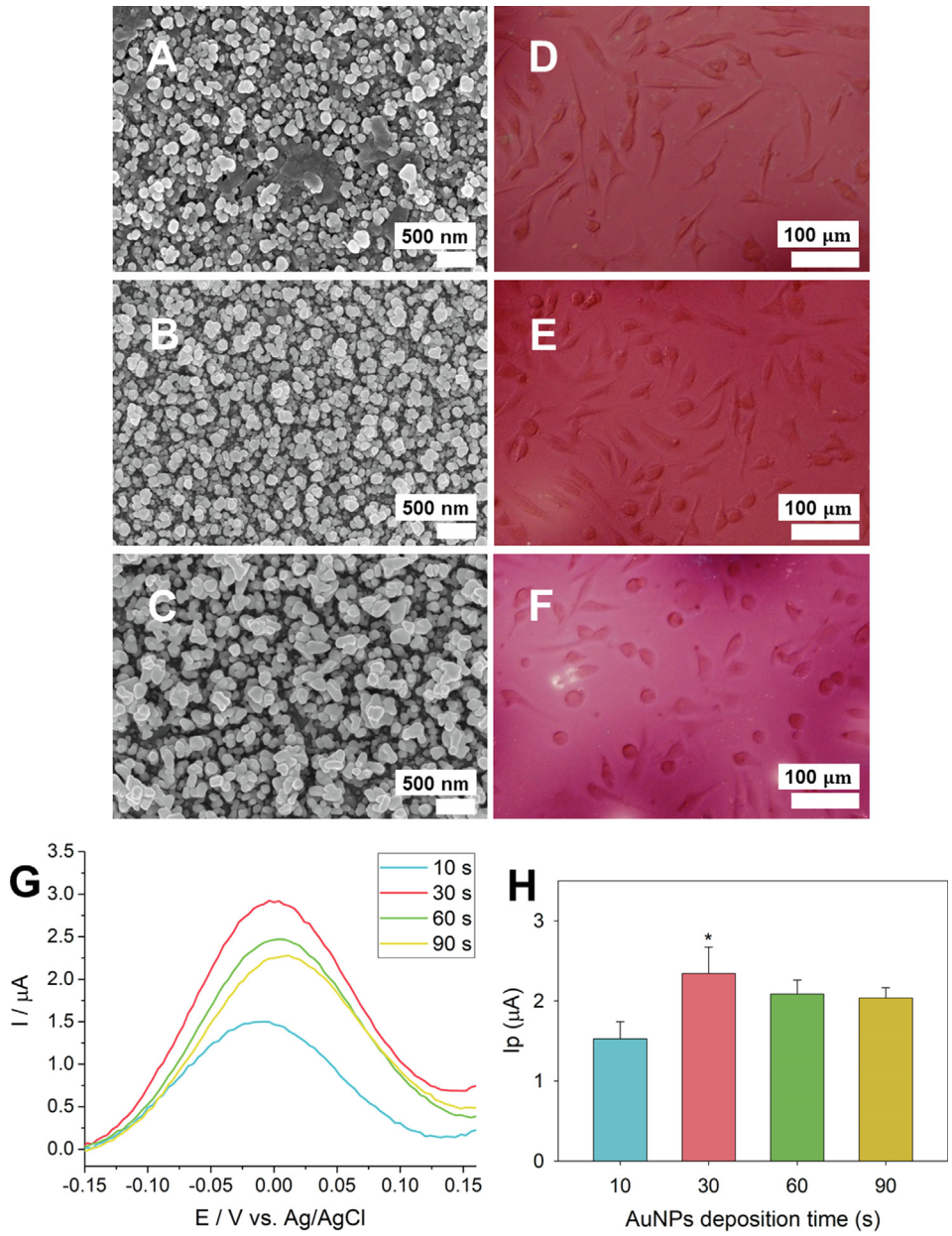

Fig. 2. SEM images of the electrochemically deposited AuNPs on the FTO electrode with electrochemical deposition times of (A) 10 s, (B) 30 s, and (C) 90 s. (D-F) Optical microscopy images of SK-MEL28 cells grown on fabricated AuNPs-FTO platforms A, B, and C, respectively. (G) DPV signals obtained from SK-MEL28 cells grown on the four different platforms according to gold deposition time. (H) The relationship between the peak current and the deposition time of AuNPs. Bars represent the mean ± s.e.m. (n = 3). Cell concentration: 8.0×10^4 cells/mL.

electrode in terms of biocompatibility. However, as shown in Fig. 2E, the cells tended to grow well on the uniformly distributed AuNPs on the electrode surface, which improved the adsorptive capacity of the biomolecules [36], showing a higher density of the attached cells than other substrates.

Next, DPV signals of the SK-MEL28 cells attached to the platforms functionalized with AuNPs were measured, and the sensitivity of the electrodes for cell detection was analyzed. Fig. 2G and H show a series of the DPV curves measured in a 1X PBS solution (pH 7.4), where the cells were incubated on four different substrates (made using different gold deposition times). A well-defined reduction peak was recorded with the platforms functionalized with AuNPs for a 30 s deposition time as compared those of other substrates. No significant signal enhancement was observed for deposition times of 60 and 90 s due to the decrease of total surface area by the larger size of AuNPs [37–39]. Based on these results, we concluded that evenly formed AuNPs with small sizes are essential to facilitate electron transfer between the target cells and the electrode surface and enhance the cell-type specific electric signals. Therefore, we chose 30 s as the AuNPs deposition time to modify the FTO electrode.

Subsequently, PLL was further modified on the AuNP/FTO substrate as a cytophilic material to enhance the biocompatibility without reducing the electrical conductance (Fig. 3). We note that the preparation of an appropriate extracellular matrix environment on the substrate is necessary for in vitro culture of mammalian cells [40]. Of the various cell adhesion molecules, we chose PLL because of its conductive nature as well as a high affinity towards mammalian cells. PLL has also been widely used for coating electrode surfaces at low concentrations to promote

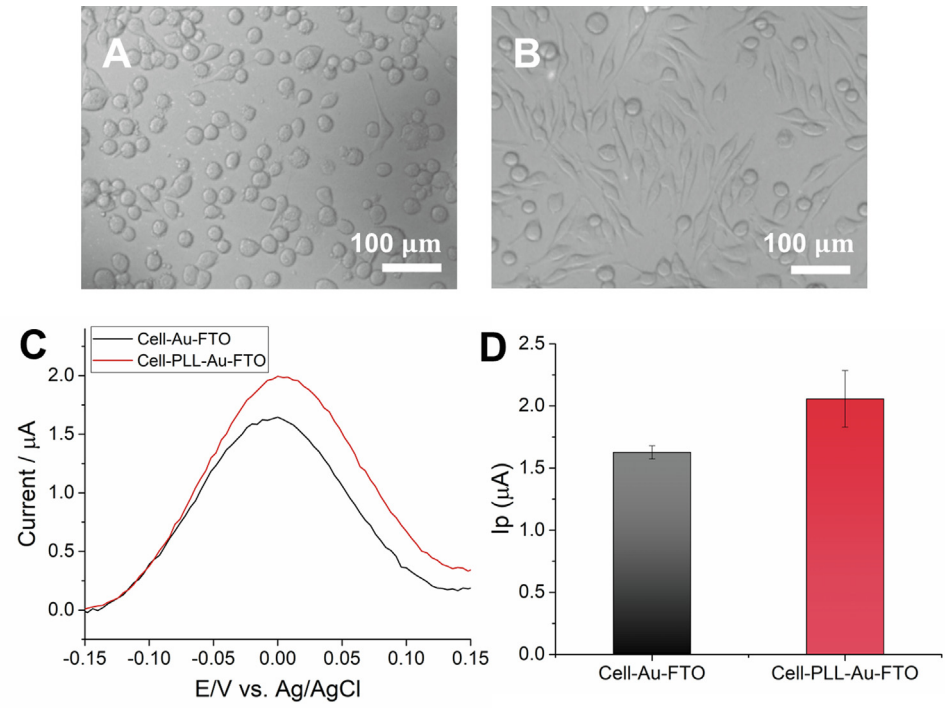

Fig. 3. (A), (B) Microscopic images of the cells grown on the (A) Au-FTO substrate and (B) PLL-Au-FTO substrate. (C) DPV signals obtained from SK-MEL28 cells grown on two different platforms according to PLL treatment. (D) The peak signals from (C). The bars represent the mean ± s.e.m. (n = 3). Cell concentration: 8.0×10^4 cells/mL.

cell attachment, with no negative effects on cell viability [41–43]. The PLL coating on conductive or semi-conductive substrates is known to encourage cells or biomolecules to interact well with the treated surfaces [44]. As shown in Fig. 3A and B, the morphologies of the cells significantly changed after PLL treatment when compared with the cells cultured on the Au-FTO substrates. Due to the PLL modification, the cellular affinity of the fabricated electrode increased, and the adherence of the cell membrane receptors (e.g., integrin) to the electrode also improved, thus broadening the attached cell area. In other words, the cell adhesion to solid substrates was promoted by electrostatic interactions between the negatively charged cell membrane and the positively charged PLL-Au-FTO substrate. As a result, the maximum peak intensity of the cells on the PLL-Au-FTO substrate was confirmed by the Ip of 2.06 μA, which was 26.4% higher than that of the non-PLL-coated Au-FTO substrate (Ip = 1.63 μA) (Fig. 3C and D). This result is attributed to the improved attachment of cells through their integrins, which function as both major adhesion receptors and linkers for biochemical signal transduction into the cells [45]. Overall, we verified that the PLL-coated AuNPs-FTO electrode is the best platform for amplifying electrical signals of skin melanoma cells in a sensitive way.

3.3. Relationship between peak current and cell numbers

The relationship between the cathodic peak current and SK-MEL28 cell number is shown in Fig. 4. Voltammetric techniques were used to measure current intensities as a function of the applied potential, and the concentration of living cancer cells was detected from voltammograms, resulting in a graph showing the correlation between the current and the potential. In the field of electrochemical cytosensors, voltammetric techniques have been widely utilized for detecting target cells due to their high sensitivity and selectivity [19]. This technology does not require sophisticated chemical reagents nor complex sample preparation, and rapidly offers reproducible information on electrodynamic processes. Fig. 4A shows a symmetrical redox peak, indicating that the redox reaction took place at the cell-electrode interface. It may be attributed to the electron transfer via the relay chain between the electrode and the buried catalytic site in the redox proteins of the living cells [46]. Since the electrochemical signals are generated from the biomolecules such as intracellular redox enzymes and metalloproteins in the cell membrane, the redox peaks increase with higher cell numbers. The voltammograms are irreversible because the lifetimes of the oxidized/reduced forms of the redox species are quite shorter than the voltammetry acquisition times [47]. As the cell number increased from 5,000 to 40,000 on the electrode, the peak current of the cells gradually increased. Fig. 4B shows the corresponding linear plot between the peak current and the number of cells. A linear relationship was established, and the correlation coefficient (R^2) between peak current and cell number was confirmed to be 0.9952, showing a clear linearity, and the quantification limit was estimated to be 2,880 cells per device. The accuracy of the method was identified by comparing it with the results of the conventional colorimetric method (Fig. 4C). The equal range of cells was cultured in the well plate, which has the same area as the fabricated electrode, and it was treated with MTT reagent. A linear relationship between the cell number and the optical density was found to have an R^2 of 0.9824, which is lower than the electrochemical method. In other words, the voltammetric response of immobilized live cancer cells can be utilized to monitor the cell population and the change in cell viability. This method has the advantages of high sensitivity, rapid measurement, non-invasive monitoring and a simple procedure as compared to a conventional assay. Table 1 shows the comparison of the electrochemical cytosensors for the detection of cancer cells. Our electrochemical cytosensor is comparable to previously reported electrochemical sensors for cancer cells. The wide linear range and low detection limit also show the large applicability and effectiveness of the developed PLL-Au modified sensor platform.

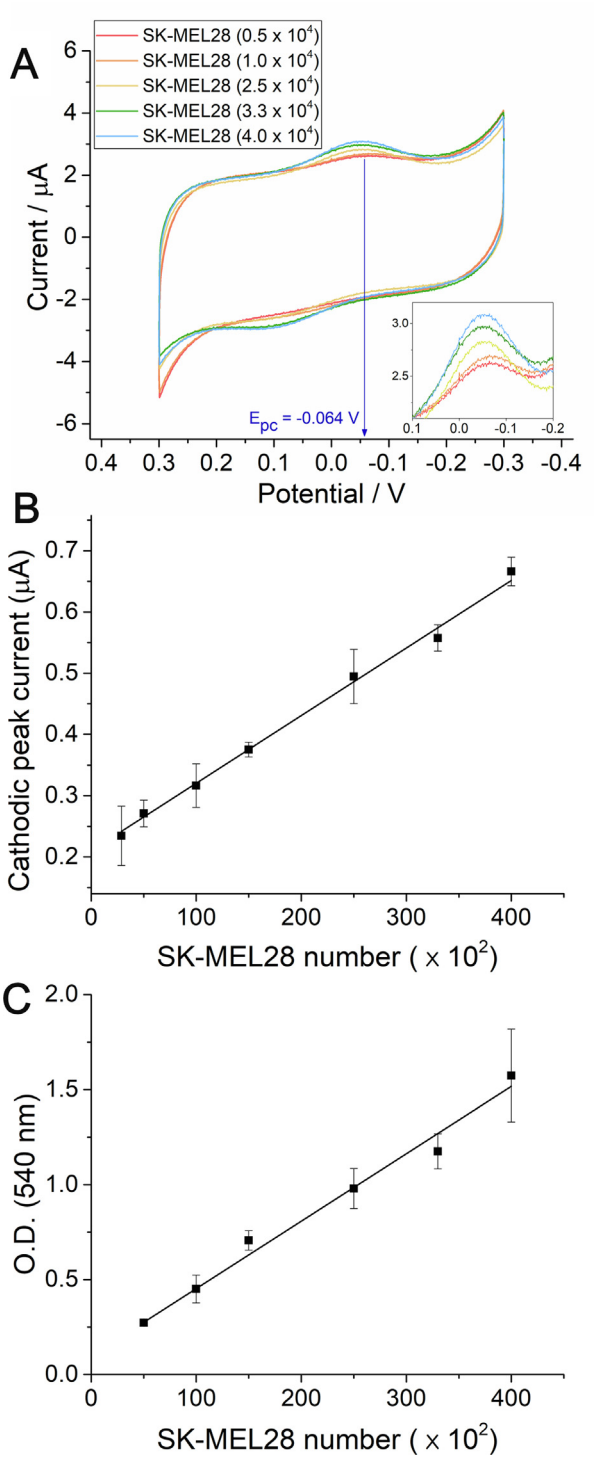

Fig. 4. Correlation analysis between cyclic voltammetry (CV) signals and the number of SK-MEL28 cells. (A) Cell number dependent alteration of CV shape and cathodic peak current (Ipc) from 0.5 $\times 10^4$, 1.0 $\times$ 10^4, 2.5 $\times$ 10^4, 3.3 $\times$ 10^4, or 4.0 $\times$ 10^4 of SK-MEL28 cells at −0.064 V (Epc: cathodic peak potential). Scan rate: 100 mV s^{-1}. (B) Scatter plot with linear regression analysis of CV cathodic peak current (Ipc) versus number of cell (n = 3, technical replicates) ($y = 0.00001x + 0.2099$, $r^2 = 0.9952$). (C) MTT viability data for the number of SK-MEL28 cells ($y = 0.00004x + 0.0975$, $r^2 = 0.9824$).

Furthermore, the reproducibility of the cytosensor was also studied. The voltammetric responses of the five electrodes fabricated with the same procedure were investigated to detect SK-MEL28 cells at the concentration of 30,000 cells per device. As shown in Fig. S2, the relative standard deviation (RSD) was calculated to be 2.03%, suggesting that the developed cytosensor has high reproducibility.

3.4. Electrochemical detection of anticancer effects of saponin on skin melanoma cells

The anticancer effect of saponin, a plant-derived chemical compound, was assessed on skin melanoma SK-MEL28 cells. As a promising agent for anticancer research, saponin has been reported to have significant anticancer activity at micromolar concentrations in some of the mammalian cell lines [48]. To explore the effect of saponin on the voltammetric response of SK-MEL28 cells, the inoculated melanoma cells were cultured on the fabricated electrodes for 2 days. Different concentrations of saponin (0–50 μM) in fresh culture medium were added for 24 h, and the DPV signal was measured. Just before the electrochemical measurement, cell culture medium was replaced with 1X PBS. Fig. 5A shows the effect of saponin on DPV responses of SK-MEL28 cells, which were found to be 0.8301 μA, 0.8261 μA, 0.6516 μA, 0.4130 μA, 0.1850 μA, and 0.1127 μA for saponin concentrations of 0, 10, 20, 30, 40, 50 μM, respectively. As the concentration of saponin increases, the cathodic peak current decreases significantly, indicating a reduction in the viability of the melanoma cells. This voltammetric variance suggested that saponin shows anticancer activity in cancer cells by inducing apoptosis. Fig. 5B shows the corresponding bar graph between the cathodic peak current and saponin concentration (conversion to cell viability: 100%, 99.5%, 78.5%, 49.7%, 22.3%, and 13.6% for 0, 10, 20, 30, 40, 50 μM, respectively). The change in the cathodic peak current of the immobilized SK-MEL28 cells on the fabricated electrode was used as a parameter for evaluating the efficiency of anticancer drugs. Moreover, electrochemical detection was carried out in a manner that was simpler and faster than the conventional colorimetric assay. To demonstrate the reliability of the developed method, anticancer drug testing based on the conventional MTT assay was conducted and compared with the electrochemical method (Fig. 5C, D). The same number of SK-MEL28 cells were seeded in the cell culture plate, and saponin was added in the same way. Fig. 5C shows the viability curves of SK-MEL28 cells for the 24 h treatment of saponin with various concentrations, which were measured to be 100%, 103.0%, 90.5%, 57.4%, 19.6%, and 6.8% for saponin concentrations of 0, 10, 20, 30, 40, and 50 μM, respectively. It was observed that the viability of SK-MEL28 cells decreased with an increase in saponin concentration. Consequently, the colorimetric result agreed with that obtained using the electrochemical method (Fig. 5D).

The cytotoxic effect of saponin on SK-MEL28 cells was further verified by cellular morphology analysis and live/dead cell staining (Fig. 6). As the concentration of saponin increased, the cells appeared to detach from the substrate, float in the culture medium, and lose their ability to organize with each other. When compared to the cells cultured at a low concentration of saponin (Fig. 6B), the cells treated with higher concentrations showed lower density and viability and failed to maintain normal functions such as adaptation and organization (Fig. 6F). Fluorescent analysis of melanoma cells was also conducted using the live/dead cell staining reagents and showed similar results as above, with the weakest green fluorescence observed for the cells exposed to the highest amount of saponin (50 μM). Taken together, the cytotoxic tendency acquired by the electrochemical method was consistent with the MTT assay and live/dead cell staining assay, which indicates that the electrochemical live cell sensing platform could be used to examine the potency of anticancer drugs in a new way.

Table 1
A comparison of the electrochemical cytosensors for detection of cancer cells.

Cell line	Substrate	Detection technique	Performance	Drug	Ref.
K562	Filter paper/punched tape/ITO glass	CV, DPV	Linear range: 2.0×10^3 to 1.0×10^7 cells mL^{-1} LOD: 1.2×10^3 cells mL^{-1}	Arsenic trioxide (As2O3), CTX	[20]
U87MG	RGD/AuNPs/ITO	CV, DPV	Linear range: 20,000 to 60,000 cells LOD: 9,379 cells/chip	Curcumin	[23]
Hela	Gold/Ti/Silicon	CV	Linear range: 8×10^4 to 2.08×10 cells	Hydroxyurea, cyclophosphamide (CTX)	[24]
MKN-28	Fibronectin/AuNPs/ITO	DPV	–	Curcumin-carrying nanoliposome	[28]
HL-60	Vicinal-dithiol-containing proteins (VDPs)@MWCNTs modified ITO	CV, DPV, EIS	Linear range: 2.7×10^2 to 2.7×10^7 cells mL^{-1} LOD: 90 cells mL^{-1}	–	[29]
HepG2	Gold/polycarbonate film	ECIS	Linear range: 1.0×10^5 to 4×10^7 cells mL^{-1}	Tamoxifen, Menadione	[49]
MCF-7	Poly calcein modified glassy carbon electroce (PCA/GCE)	CV, LSV	Linear range: 3.0×10^3 to 7.0×10^6 cells mL^{-1} LOD: 3,000 cells mL^{-1}	CTX	[50]
PC-3	Multiwalled carbon nanotubes modified GCE	CV	Nonlinear range: 1.0×10^5 to 8×10^6 cells mL^{-1}	–	[51]
SK-MEL28	PLL/AuNPs/FTO	CV, DPV	Linear range: 2,880 to 40,000 cells LOD: 2,880 cells	Saponin	This work

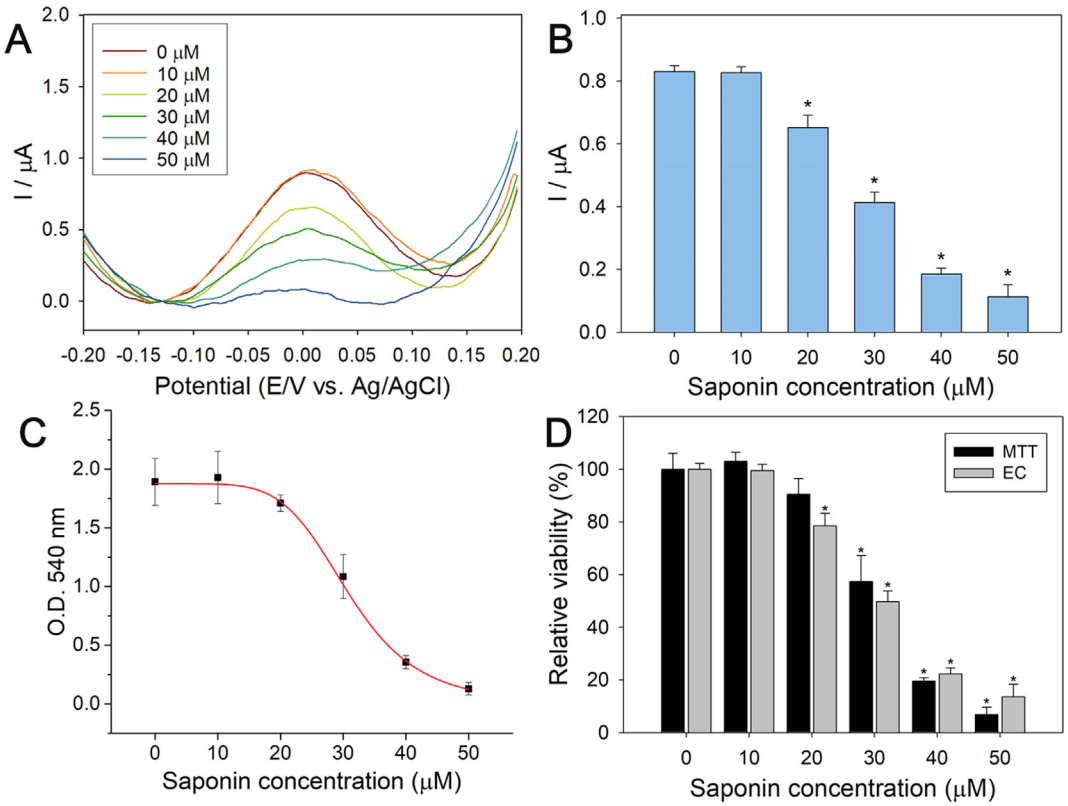

Fig. 5. Representative results of in vitro anticancer study for saponin in SK-MEL28 cells. (A) DPV curves of SK-MEL28 cells treated with saponin at various concentrations. (B) DPV peak current obtained from (A) are presented as a bar graph. (C) MTT assay was performed to determine cell viability after saponin treatment. The regression curve was fitted to the data ($r^2 = 0.9985$). (D) Viability graphs for the effect of saponin on the malignant melanoma SK-MEL28 cells obtained with a MTT assay and the proposed electrochemical method.

4. Conclusion

In this study, we developed an electrochemical cytosensor for cancer cell detection and evaluation of anticancer effects of saponin on skin malignant melanoma cells (SK-MEL28 cell line). The electrodeposition of AuNPs onto the FTO substrate, with an additional modification of positively charged amino acids (PLL), remarkably boosted the detection sensitivity. The platform was able to detect melanoma cells within a linear range of 2,880–40,000 cells/device, which was greater than the conventional

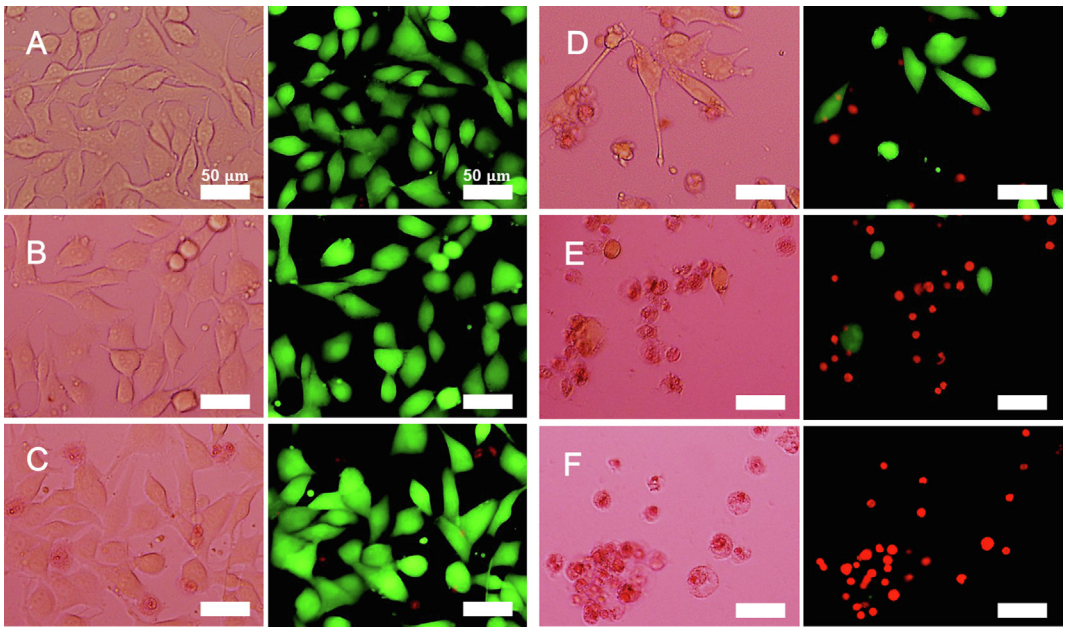

Fig. 6. Fluorescent microscopy images of SK-MEL28 cells treated with (A) 0, (B) 10, (C) 20, (D) 30, (E) 40, and (F) 50 μM saponin for 24 h that were and stained with calcein-AM/EthD-1. Green: live cells; Red: dead or dying cells.

colorimetric assay in terms of sensitivity (LOQ: 2,880 cells/device) and detection time (<2 min). Moreover, the cytotoxicity of an anticancer drug, saponin, was evaluated using the electrochemical sensing platform, and the result was consistent with methods such as MTT assay and cell staining assay, leading us to conclude that the cytosensor can be used for toxicity assessments of anticancer drugs. Thus, the developed electrochemical cytosensor will be a promising approach for screening the anticancer effects of various chemical/natural compounds and has potential to be extended to detect other cancer-related cells or biomarkers in clinical analysis.

Declaration of Competing Interest

The authors declare that they have no known competing financial interests or personal relationships that could have appeared to influence the work reported in this paper.

Acknowledgements

This research was supported by the Basic Science Research Program through the National Research Foundation (NRF) (of Korea), South Korea (2018R1A6A1A03024231, 2021R1A2C1003566, 2018H1A2A1060864-Global Ph.D. Fellowship Program).

Appendix A. Supplementary material

Supplementary data to this article can be found online at https://doi.org/10.1016/j.bioelechem.2021.107813.

References

[1] R.L. Siegel, K.D. Miller, A. Jemal, Cancer statistics, 2020, CA: Cancer J. Clin. 70 (1) (2020) 7–30.
[2] J. D'Orazio, S. Jarrett, A. Amaro-Ortiz, T. Scott, UV radiation and the skin, Int. J. Mol. Sci. 14 (6) (2013) 12222–12248.
[3] K.T. Flaherty, Targeting metastatic melanoma, Annu. Rev. Med. 63 (2012) 171–183.
[4] J.A. Sosman, K.B. Kim, L. Schuchter, R. Gonzalez, A.C. Pavlick, J.S. Weber, G.A. McArthur, T.E. Hutson, S.J. Moschos, K.T. Flaherty, Survival in BRAF V600–mutant advanced melanoma treated with vemurafenib, N. Engl. J. Med. 366 (8) (2012) 707–714.
[5] F.S. Hodi, S.J. O'Day, D.F. McDermott, R.W. Weber, J.A. Sosman, J.B. Haanen, R. Gonzalez, C. Robert, D. Schadendorf, J.C. Hassel, Improved survival with ipilimumab in patients with metastatic melanoma, N. Engl. J. Med. 363 (8) (2010) 711–723.
[6] Z. Liu, B. Delavan, R. Roberts, W. Tong, Lessons learned from two decades of anticancer drugs, Trends Pharmacol. Sci. 38 (10) (2017) 852–872.
[7] S. Bose, S. Banerjee, A. Mondal, U. Chakraborty, J. Pumarol, C.R. Croley, A. Bishayee, Targeting the JAK/STAT signaling pathway using phytocompounds for cancer prevention and therapy, Cells 9 (6) (2020) 1451.
[8] K. El-Bayoumy, R. Sinha, Mechanisms of mammary cancer chemoprevention by organoselenium compounds, Mutat. Res./Fundam. Mol. Mech. Mutagen. 551 (1–2) (2004) 181–197.
[9] L.-R. Sun, W. Zhou, H.-M. Zhang, Q.-S. Guo, W. Yang, B.-J. Li, Z.-H. Sun, S.-H. Gao, R.-J. Cui, Modulation of multiple signaling pathways of the plant-derived natural products in cancer, Front. Oncol. 9 (2019).
[10] Y. Tu, L. Chen, N. Ren, B. Li, Y. Wu, G.O. Rankin, Y. Rojanasakul, Y. Wang, Y.C. Chen, Standardized saponin extract from baiye no. 1 Tea (Camellia sinensis) flowers induced S phase cell cycle arrest and apoptosis via AKT-MDM2-p53 signaling pathway in ovarian cancer cells, Molecules 25 (15) (2020) 3515.
[11] S. Man, W. Gao, Y. Zhang, L. Huang, C. Liu, Chemical study and medical application of saponins as anti-cancer agents, Fitoterapia 81 (7) (2010) 703–714.
[12] D. Wang, R. Huo, C. Cui, Q. Gao, J. Zong, Y. Wang, Y. Sun, R. Hou, Anticancer activity and mechanism of total saponins from the residual seed cake of Camellia oleifera Abel. in hepatoma-22 tumor-bearing mice, Food Funct. 10 (5) (2019) 2480–2490.
[13] P. Koczurkiewicz, K. Klaś, K. Grabowska, K. Piska, K. Rogowska, K. Wójcik-Pszczoła, I. Podolak, A. Galanty, M. Michalik, E. Pękala, Saponins as chemosensitizing substances that improve effectiveness and selectivity of anticancer drug—Minireview of in vitro studies, Phytother. Res. 33 (9) (2019) 2141–2151.
[14] K. Ock, W.I. Jeon, E.O. Ganbold, M. Kim, J. Park, J.H. Seo, K. Cho, S.-W. Joo, S.Y. Lee, Real-time monitoring of glutathione-triggered thiopurine anticancer drug release in live cells investigated by surface-enhanced Raman scattering, Anal. Chem. 84 (5) (2012) 2172–2178.
[15] M.A. Kafi, C.-H. Yea, T.-H. Kim, A.K. Yagati, J.-W. Choi, Electrochemical cell chip to detect environmental toxicants based on cell cycle arrest technique, Biosens. Bioelectron. 41 (2013) 192–198.
[16] S.S. Panikar, G. Ramírez-García, S. Sidhik, T. Lopez-Luke, C. Rodriguez-Gonzalez, I.H. Ciapara, P.S. Castillo, T. Camacho-Villegas, E. De la Rosa, Ultrasensitive SERS substrate for label-free therapeutic-drug monitoring of paclitaxel and cyclophosphamide in blood serum, Anal. Chem. 91 (3) (2018) 2100–2111.
[17] H.-W. Kang, H. Muramatsu, B.-J. Lee, Y.-S. Kwon, Monitoring of anticancer effect of cisplatin and 5-fluorouracil on HepG2 cells by quartz crystal microbalance and micro CCD camera, Biosens. Bioelectron. 26 (4) (2010) 1576–1581.
[18] R. Maruhashi, H. Eguchi, R. Akizuki, S. Hamada, T. Furuta, T. Matsunaga, S. Endo, K. Ichihara, A. Ikari, Chrysin enhances anticancer drug-induced toxicity

mediated by the reduction of claudin-1 and 11 expression in a spheroid culture model of lung squamous cell carcinoma cells, Sci. Rep. 9 (1) (2019) 1–14.
[19] F. Vajhadin, S. Ahadian, J. Travas-Sejdic, J. Lee, M. Mazloum-Ardakani, J. Salvador, G.E. Aninwene II, P. Bandaru, W. Sun, A. Khademhossieni, Electrochemical cytosensors for detection of breast cancer cells, Biosens. Bioelectron. 151 (2020) 111984.
[20] C. Yu, Z. Zhu, L. Wang, Q. Wang, N. Bao, H. Gu, A new disposable electrode for electrochemical study of leukemia K562 cells and anticancer drug sensitivity test, Biosens. Bioelectron. 53 (2014) 142–147.
[21] X. Guo, Q. Wang, J. Li, J. Cui, S. Zhou, S. Hao, D. Wu, A mini-electrochemical system integrated micropipet tip and pencil graphite electrode for detection of anticancer drug sensitivity in vitro, Biosens. Bioelectron. 64 (2015) 594–596.
[22] C.-H. Yea, H.-C. Jeong, S.-H. Moon, M.-O. Lee, K.-J. Kim, J.-W. Choi, H.-J. Cha, In situ label-free quantification of human pluripotent stem cells with electrochemical potential, Biomaterials 75 (2016) 250–259.
[23] I.R. Suhito, W. Lee, S. Baek, D. Lee, J. Min, T.-H. Kim, Rapid and sensitive electrochemical detection of anticancer effects of curcumin on human glioblastoma cells, Sens. Actuators, B 288 (2019) 527–534.
[24] W.A. El-Said, C.-H. Yea, H. Kim, B.-K. Oh, J.-W. Choi, Cell-based chip for the detection of anticancer effect on HeLa cells using cyclic voltammetry, Biosens. Bioelectron. 24 (5) (2009) 1259–1265.
[25] Y. Zhao, D. Huo, J. Bao, M. Yang, M. Chen, J. Hou, H. Fa, C. Hou, Biosensor based on 3D graphene-supported Fe3O4 quantum dots as biomimetic enzyme for in situ detection of H2O2 released from living cells, Sens. Actuators, B 244 (2017) 1037–1044.
[26] F. Yan, J. Chen, H. Ju, Immobilization and electrochemical behavior of gold nanoparticles modified leukemia K562 cells and application in drug sensitivity test, Electrochem. Commun. 9 (2) (2007) 293–298.
[27] Y. Ye, J. Ji, Z. Sun, P. Shen, X. Sun, Recent advances in electrochemical biosensors for antioxidant analysis in foodstuff, TrAC, Trends Anal. Chem. 122 (2020) 115718.
[28] N. Angeline, I.R. Suhito, C.-H. Kim, G.-P. Hong, C.G. Park, S.H. Bhang, Z. Luo, T.-H. Kim, A fibronectin-coated gold nanostructure composite for electrochemical detection of effects of curcumin-carrying nanoliposomes on human stomach cancer cells, Analyst 145 (2) (2020) 675–684.
[29] Y. Xu, H. Wu, C. Huang, C. Hao, B. Wu, C. Miao, S. Chen, N. Jia, Sensitive detection of tumor cells by a new cytosensor with 3D-MWCNTs array based on vicinal-dithiol-containing proteins (VDPs), Biosens. Bioelectron. 66 (2015) 321–326.
[30] F.A. Armstrong, G.S. Wilson, Recent developments in faradaic bioelectrochemistry, Electrochim. Acta 45 (15–16) (2000) 2623–2645.
[31] M.D. Sternlicht, Z. Werb, How matrix metalloproteinases regulate cell behavior, Annu. Rev. Cell Dev. Biol. 17 (1) (2001) 463–516.
[32] A.J. Gates, G.L. Kemp, C.Y. To, J. Mann, S.J. Marritt, A.G. Mayes, D.J. Richardson, J. N. Butt, The relationship between redox enzyme activity and electrochemical potential—cellular and mechanistic implications from protein film electrochemistry, PCCP 13 (17) (2011) 7720–7731.
[33] E. Paleček, J. Tkáč, M. Bartosik, T.s. Bertók, V. Ostatná, J. Paleček, Electrochemistry of nonconjugated proteins and glycoproteins. Toward sensors for biomedicine and glycomics, Chem. Rev. 115 (5) (2015) 2045–2108.
[34] X. Wang, R. Xu, X. Sun, Y. Wang, X. Ren, B. Du, D. Wu, Q. Wei, Using reduced graphene oxide-Ca: CdSe nanocomposite to enhance photoelectrochemical activity of gold nanoparticles functionalized tungsten oxide for highly sensitive prostate specific antigen detection, Biosens. Bioelectron. 96 (2017) 239–245.
[35] J.-X. Liu, X.-L. Liang, F. Chen, S.-N. Ding, Ultrasensitive amperometric cytosensor for drug evaluation with monitoring early cell apoptosis based on Cu2O@ PtPd nanocomposite as signal amplified label, Sens. Actuators, B 300 (2019) 127046.
[36] M. Roushani, S. Farokhi, Efficient determination of butylated hydroxyanisole using an electrochemical sensor based on cobalt oxide nanoparticles modified electrode, Anal. Bioanal. Chem. Res. 3 (1) (2016) 101–110.
[37] X. Dai, R.G. Compton, Direct electrodeposition of gold nanoparticles onto indium tin oxide film coated glass: application to the detection of arsenic (III), Anal. Sci. 22 (4) (2006) 567–570.
[38] Y. Xu, W. Zhang, J. Shi, X. Zou, Y. Li, T.H. Elrasheid, X. Huang, Z. Li, X. Zhai, X. Hu, Electrodeposition of gold nanoparticles and reduced graphene oxide on an electrode for fast and sensitive determination of methylmercury in fish, Food Chem. 237 (2017) 423–430.
[39] D. Buttard, F. Oelher, T. David, Gold colloidal nanoparticle electrodeposition on a silicon surface in a uniform electric field, Nanoscale Res. Lett. 6 (1) (2011) 580.
[40] G.A. Hudalla, W.L. Murphy, Chemically well-defined self-assembled monolayers for cell culture: toward mimicking the natural ECM, Soft Matter 7 (20) (2011) 9561–9571.
[41] L.M. Ricles, S.Y. Nam, K. Sokolov, S.Y. Emelianov, L.J. Suggs, Function of mesenchymal stem cells following loading of gold nanotracers, Int. J. Nanomed. 6 (2011) 407.
[42] B. Huang, N. Jia, L. Chen, L. Tan, S. Yao, Electrochemical impedance spectroscopy study on polymerization of L-lysine on electrode surface and its application for immobilization and detection of suspension cells, Anal. Chem. 86 (14) (2014) 6940–6947.
[43] A. Blau, Cell adhesion promotion strategies for signal transduction enhancement in microelectrode array in vitro electrophysiology: An introductory overview and critical discussion, Curr. Opin. Colloid Interface Sci. 18 (5) (2013) 481–492.
[44] S. Nilsson, N.D. Robinson, On the anodic deposition of poly-L-lysine on indium tin oxide, Electrochim. Acta 196 (2016) 629–633.
[45] R.O. Hynes, Integrins: bidirectional, allosteric signaling machines, Cell 110 (6) (2002) 673–687.
[46] H.A. Reeve, P.A. Ash, H. Park, A. Huang, M. Posidias, C. Tomlinson, O. Lenz, K.A. Vincent, Enzymes as modular catalysts for redox half-reactions in H2-powered chemical synthesis: from biology to technology, Biochem. J 474 (2) (2017) 215–230.
[47] E.M. Espinoza, J.A. Clark, J. Soliman, J.B. Derr, M. Morales, V.I. Vullev, Practical aspects of cyclic voltammetry: how to estimate reduction potentials when irreversibility prevails, J. Electrochem. Soc. 166 (5) (2019) H3175.
[48] X.-H. Xu, T. Li, C.M.V. Fong, X. Chen, X.-J. Chen, Y.-T. Wang, M.-Q. Huang, J.-J. Lu, Saponins from Chinese medicines as anticancer agents, Molecules 21 (10) (2016) 1326.
[49] J.H. Yeon, J.-K. Park, Cytotoxicity test based on electrochemical impedance measurement of HepG2 cultured in microfabricated cell chip, Anal. Biochem. 341 (2) (2005) 308–315.
[50] X. Guo, J. Li, J. Cui, Y. Wang, H. Gao, S. Hao, D. Wu, Sensitive detection of MCF-7 cells based on poly calcein modified electrode and its applied in cytotoxicity assay, Int. J. Electrochem. Sci. 10 (2015) 6732–6742.
[51] D.-M. Wu, G.-L. Fu, H.-Z. Fang, L. Hu, J.-L. Li, X. Yuan, Z.-Y. Zhang, Studies on the origin of the voltammetric response of the PC-3 cell suspension, Talanta 78 (2) (2009) 602–607.